Inorg. Chem. **2003**, *42*, 3884–3890

^{11}B, ^{23}Na, ^{27}Al, and ^{19}F NMR Study of Solid and Molten Na_3AlF_6–$Na_2B_4O_7$

Catherine Bessada*,† and Elena M. Anghel‡

CNRS, Centre de Recherche sur les Matériaux à Hautes Températures, 1D, Avenue de la Recherche Scientifique, 45071 Orléans Cedex 2, France, and Institute of Physical Chemistry "I.G.Murgulescu" of Romanian Academy of Science, Spl. Independentei 202, 77208 Bucharest, Romania

Received October 1, 2002

High temperature electrochemical synthesis is a very promising method for the production of refractory boride powders and coatings. The $Na_2B_4O_7$–Na_3AlF_6 binary system is part of the more complex NaCl–Na_3AlF_6–$Na_2B_4O_7$–TiO_2 electrolyte proposed for TiB_2 electrosynthesis. A new approach by high temperature and high resolution solid state nuclear magnetic resonance was employed for the structural description of this system, from the solid at room temperature to the liquid at 1100 °C. The change in ^{27}Al, ^{23}Na, ^{11}B, and ^{19}F NMR spectra with composition give evidence for the insertion of aluminum into the glassy network of $Na_2B_4O_7$ as $[AlO_4]$ and diluted $[AlF_6]$ units as well as formation of $[BOF_2]$ groups into solidified mixtures. A devitrification mechanism of glassy $Na_2B_4O_7$ under influence of Na_3AlF_6 addition and temperature was discussed in terms of lowering boron coordination and obtaining oxyfluoride species.

Introduction

Titanium diboride (TiB_2) powder has several unique properties, particularly its high melting point (2980 °C), high electrical conductivity, hardness, and chemical stability toward attack by corrosive molten fluorides and molten metals. It is thus an excellent precursor for obtaining high temperature structural ceramic composites with many applications. These include use in heat exchangers, as wear resistant elements in cutting tools and forming dies, and cathodes in Hall−Heroult cells for the electrolytic production of aluminum.[1−3] Among the different methods of boride production, the high temperature electrochemical synthesis of TiB_2 powder with controlled particle size in molten Na_3AlF_6−NaCl electrolyte containing oxygenated compounds of titanium (TiO_2) and boron ($Na_2B_4O_7$) has proved promising for many years.[3] However, the electrosynthesis mechanism in the production of TiB_2 has not been elucidated due to inadequate structural information. It was previously proposed[4] that the electrosynthesis mechanism in this oxo-fluoro-electrolyte involved the cathodic discharge of BF_4^- and TiF_6^{2-} anions. Our preliminary work[5,6] using IR and Raman spectroscopy to investigate structural aspects of the $Na_2B_4O_7$−Na_3AlF_6 system revealed the modifier role of Na_3AlF_6 for the vitreous structure of $Na_2B_4O_7$ by the formation of new BF_4^- and/or BO_3F^{4-} anions as a result of the appropriate substitution of O^{2-} and F^-. Further, in a lower concentration range of $Na_2B_4O_7$ (20−60 wt %), anionic complexes $AlF_x^{(x-3)-}$ ($x = 6$, 5, and 4) were thought to coexist in melts. However, further structural information by NMR spectroscopy is required to understand the mechanism of devitrification of the borate structure as Na_3AlF_6 content is increased.

The current understanding of the local structure of borate systems, extensively investigated by NMR spectroscopy, usually considers only alkali borate and borosilicate glasses.[7,8] When fluorine is incorporated into the borate glass network,

* Corresponding author. E-mail: bessada@cnrs-orleans.fr. Fax: +33(0) 238 638 103.
† CNRS, Centre de Recherche sur les Matériaux à Hautes Températures.
‡ Institute of Physical Chemistry "I.G.Murgulescu" of Romanian Academy of Science.

(1) Kutznetsov, S. A. *Russ. J. Electrochem.* **1999**, *35*, 1143−1158.
(2) Ene, N. *Rev. Roum. Chim.* **1999**, *7*, 643−650. Devyatkin, S. V.; Kaptay, G. *J. Solid State Chem.* **2000**, *154*, 107−109. Brodkin, D.; Zavaliangos, A.; Kalidinki, S. R.; Barsoum, M. *J. Am. Ceram. Soc.* **1999**, *82*, 665−672. Jones, A. H.; Trueman, C.; Dobedoe, J.; Huddleston, J.; Lewis, M. H. *Br. Ceram. Trans. J.* **2001**, *100*, 49−54.
(3) Gomes, J. N.; Uchida, K. U.S. Patent 3.775.271, 1972.
(4) Makyta, M.; Danek, V.; Haarberg, G. M.; Thonstad, J. *J. Appl. Electrochem.* **1996**, *26*, 319−324.
(5) Anghel, E. M.; Zaharescu, M.; Zuca, S.; Pavlatou, E. *J. Mater. Sci.* **1999**, *34*, 3923−3929.
(6) Anghel, E. M.; Bessada, C.; Zuca, S.; Pavlatou, E. *Progress in Molten Salts Chemistry*; Berg, R. W., Hjuler, H. A., Eds.; Elsevier: New York, 2000; Vol. 1, pp 59−63.
(7) Bray, P. J. *Inorg. Chim. Acta* **1999**, *289*, 158−173.
(8) Sen, S. *J. Non-Cryst. Solids* **1999**, *253*, 84−94.

10.1021/ic026074o CCC: $25.00
Published on Web 05/10/2003

one or two oxygen atoms in the BO_4 and BO_3 configurations can be replaced by fluorine and lead to $B(O,F)_4$ and $B(O,F)_3$ units that are associated with ^{11}B NMR line shape modifications.[9,10] This partial substitution of fluoride for oxide can cause a significant lowering in melt viscosity and increased diffusion coefficients, features that are important for the electrolyte when planning to obtain TiB_2. From ^{11}B MAS experiments at room temperature, the relative proportion of four- and three-coordinated boron (N_4/N_3 ratio) species can be easily quantified, the former ones correlated with a glassy structure.

From solid state ^{27}Al and ^{23}Na MAS spectra, the coordination state and local symmetry of the different structural units can be quantitatively determined. Empirical correlations established between experimental chemical shifts and structural parameters now allow us to discriminate between different Al−O and Al−F configurations. Accordingly, the ^{27}Al chemical shifts of oxides fall into well separated ranges: 50−90, 35−40, and ±20 ppm for AlO_4, AlO_5, and AlO_6, respectively, while aluminum atoms in solid alkali fluoroaluminates are essentially octahedrally coordinated with F. Also, the reported ^{27}Al chemical shift range lies between −15 and +1.4 ppm, at least 20 ppm more shielded than AlO_6 octahedra in aluminum oxides.[11,12]

As TiB_2 electrosynthesis develops in the molten electrolyte, NMR measurements in situ at high temperature are crucial for understanding the structural changes occurring in the molten phase, not only from the practical point of view but also from fundamental considerations. High temperature ^{27}Al NMR studies[13−15] in molten alkali fluoroaluminates have extended the known set of chemical shift values to well separated ranges for the AlF_4, AlF_5, and AlF_6 configurations. The ^{27}Al NMR spectra obtained for equimolar mixtures of $MF-AlF_3$ (M = Li, Na, K) evidenced a chemical shift range for AlF_4 coordination between 34 and 45 ppm.[15]

Conversely, empirical correlations, between average Na−O and Na−F bond lengths and the ^{23}Na isotropic chemical shift in crystalline oxide and fluoride compounds, can also be used to understand better the development of structure in molten materials.[16−18]

Although the similarity between the glass and the corresponding melt structure is still in debate,[19,20] using the line width and position of in situ high temperature spectra, structural development, and species exchange can be explored in these liquids. Peaks narrow significantly when the viscosity of the liquid becomes sufficiently low and allows rapid reorientation of structural units and averaging of the quadrupolar broadening to occur.[8]

In this study, we examine the mutual influence of the two components on each other structure, the modifying effect at low content of cryolite, and the development of boron and aluminum speciation to form new oxyfluoro species.

Table 1. Nominal Composition of Investigated Binary Mixtures $Na_3AlF_6-Na_2B_4O_7$

sample	wt %	mol %
0 B	100:0	100:0
20 B	80:20	79.31:20.69
40 B	60:40	58.97:41.03
60 B	40:60	38.98:61.02
80 B	20:80	19.32:80.68
100 B	0:100	0:100

Experimental Section

Sample Preparation. $NaBF_4$ (Acros) of 98% purity, reagent grade Na_3AlF_6 (Merck), and $Na_2B_4O_7{\cdot}10H_2O$ (Reactivul Bucharest) were used as supplied. Anhydrous $Na_2B_4O_7$ (sodium diborate) was obtained by slow dehydration of $Na_2B_4O_7{\cdot}10H_2O$ (Borax) at 320 °C and subsequent heating of the salt up at 900 °C for 10 min. The appropriate mixtures were homogenized, melted, quenched, and stored in a drybox. Six different compositions of the binary system $Na_2B_4O_7-Na_3AlF_6$, Table 1, were studied.

Nuclear Magnetic Resonance Spectroscopy. All the NMR spectra were recorded using a Bruker DSX 400 NMR spectrometer, operating at 128.3, 104.2, 105.8, and 376.4 MHz for ^{11}B, ^{27}Al, ^{23}Na, and ^{19}F, respectively.

Room temperature magic angle spinning (MAS) NMR spectra were acquired with a high speed MAS NMR probe (Bruker). Finely ground samples were spun at 35 kHz in 2.5 mm ZrO_2 rotors, previously filled in a glovebox. All spectra were measured with short pulse excitations, using a typical 0.5 μs pulse length for ^{11}B, ^{27}Al, and ^{23}Na and 1.2 μs for ^{19}F, recycle delays of 1 s, and spectral widths of 1 MHz. Free induction decays (FIDs) from 1024 to 2048 were collected to obtain a good signal-to-noise ratio. Owing to long relaxation times, ^{19}F measurements were carefully adjusted in order to avoid any saturation of the signal. The recycle delays were typically of few seconds, and the pulse durations were lowered ($\pi/6$).

In situ high temperature NMR static spectra were obtained using the high temperature laser heated system developed at CRMHT-CNRS in Orleans (France), previously described.[13]

The various spectra were acquired using a single pulse sequence, with $\pi/2$ pulses, a recycle delay of 1 s, and 8−128 accumulations. Samples, 70−75 mg, in an argon drybox were placed in a boron nitride, BN, crucible and tightly closed by a screw cap. The samples were melted and heated directly up to 1030 °C and their spectra collected on cooling. To limit evaporation and melt composition change, measurements were limited to 5 min duration at each temperature. ^{23}Na and ^{27}Al spectra were recorded in succession

(9) Jäger, C.; Haubenreisser, U. *Phys. Chem. Glasses* **1985**, *26*, 152−156.
(10) Boussard-Pledel, C.; Le Floch, M.; Fonteneau, G.; Lucas, J.; Sinbandhit, S.; Shao, J.; Angell, C. A.; Emery, J.; Buzare, J. Y. *J. Non-Cryst. Solids* **1997**, *209*, 247−256.
(11) Dirken, P. J.; Jansen, J. B. H.; Schuiling, R. D. *Am. Mineral.* **1992**, *77*, 718−724.
(12) Müller, D.; Bentrup, U. *Z. Anorg. Allg. Chem.* **1989**, *575*, 17−25.
(13) Lacassagne, V.; Bessada, C.; Florian, P.; Bouvet, S.; Ollivier, B.; Coutures, J.-P.; Massiot, D. *J. Phys. Chem. B* **2002**, *106* (8), 1862−1868.
(14) Robert, E.; Lacassagne, V.; Bessada, C.; Massiot, D.; Gilbert, B.; Coutures, J.-P. *Inorg. Chem.* **1999**, *38*, 214−217.
(15) Bessada, C.; Lacassagne, V.; Massiot, D.; Florian, P.; Coutures, J.-P.; Robert, E.; Gilbert, B. *Z. Naturforsch.* **1999**, *54a*, 162−166.
(16) George, A. M.; Sen, S.; Stebbins, J. F. *Solid State Nucl. Magn. Reson.* **1997**, *10*, 9−17.
(17) Du, L.-S.; Samoson, A.; Tuherm, T.; Grey, C. *Chem. Mater.* **2000**, *12*, 3611−3616.
(18) Koller, H.; Enghelhardt, G.; Kentgens, A. P. M.; Sauer, J. *J. Phys. Chem.* **1994**, *98*, 1544−1551.
(19) Van Wüllen, L.; Müller-Warmuth, W. *Solid State Commun.* **1993**, *2*, 279−284.
(20) Handa, K.; Kita, Y.; Kohara, S.; Suzuya, K.; Fukunaga, T.; Misawa, M.; Iida, T.; Iwasaki, H.; Umesaki, N. *J. Phys. Chem. Solids* **1999**, *60*, 1465−1471.

while ^{19}F and ^{11}B spectra were obtained from a fresh sample under the same conditions.

The reported high temperature ^{11}B spectra required correction from a broad probe-head signal due to the presence of boron in the crucible material (BN) as well as in the probe assembly. The temperatures reported here are accurate within ±5 °C. The various ^{27}Al, ^{23}Na, ^{11}B, and ^{19}F chemical shifts were referenced to 1 M aqueous solutions of $Al(NO_3)_3$, NaCl, $(C_2H_5)_2OBF_3$, and $CFCl_3$, respectively.

The ^{27}Al, ^{23}Na, and ^{11}B MAS NMR spectra are characteristic of quadrupolar nuclei ($I = {}^5/_2$ and ${}^3/_2$). The MAS spectrum of the glass consists of an asymmetric broad line corresponding to the central $\langle -{}^1/_2 \leftrightarrow {}^1/_2 \rangle$ transition and spinning sidebands arising from the outer $\langle \pm{}^3/_2 \leftrightarrow \pm{}^1/_2 \rangle$ transitions (the $\langle \pm{}^5/_2 \leftrightarrow \pm{}^3/_2 \rangle$ transitions are generally too wide to be detected). The isotropic chemical shift and the quadrupolar coupling constant, as well as the relative population of the boron bearing units, B_{III} and B_{IV}, were calculated according to previously discussed protocols, employing the software Dmfit developed by D. Massiot (CNRS, Orléans, France).[21]

Results and Discussion

MAS NMR Spectra at Room Temperature. The fast MAS NMR spectra, obtained for the nuclei ^{27}Al, ^{23}Na, ^{11}B, and ^{19}F at room temperature, showed the local development of $Na_2B_4O_7-Na_3AlF_6$ solidified melts. Thus, all ^{27}Al MAS spectra recorded (Figure 1A) consist of an intense symmetric line at 0 ppm with spinning sidebands associated with a relatively low quadrupolar interaction (QCC ≈ 2.3 MHz), assignable to the AlF_6^{3-} octahedral site in solid cryolite, and a more asymmetric peak, with a typical quadrupolar shape. This latter contribution, associated with a high quadrupolar coupling constant (QCC ≈ 8.7 MHz) and an isotropic chemical shift at 75 ppm, can be unambiguously assigned to AlO_4^- units. Figure 1B reports the modeling of the 80 B spectrum, with the decomposition in two distinct quadrupolar contributions.[21]

Insertion of Al in the glassy borate network is thus clearly shown in the spectrum of the 80 wt % $Na_2B_4O_7$ mixture, 80 B, where the peak corresponding to the AlF_6^{3-} site exhibits a typical dissymmetric shape with a sharp left edge and a trailing right edge,[22] the general case for amorphous ^{27}Al spectra, and this band is hence associated with a distribution of the NMR parameters due to a disordered environment.[23] This behavior was earlier[5] noted in the IR spectra of binary mixtures with high $Na_2B_4O_7$ content, where it was suggested that AlF_6^{3-} anions were diluted in the glassy diborate matrix. For samples with a higher content of Na_3AlF_6, the ^{27}Al spectra are just the superposition of the cryolite and AlO_4 signals. However, no visible increase in relative intensity was observed for the oxide peak, compared with the 80 B spectrum. The concentration of the aluminum contribution to this signal is around 10%.

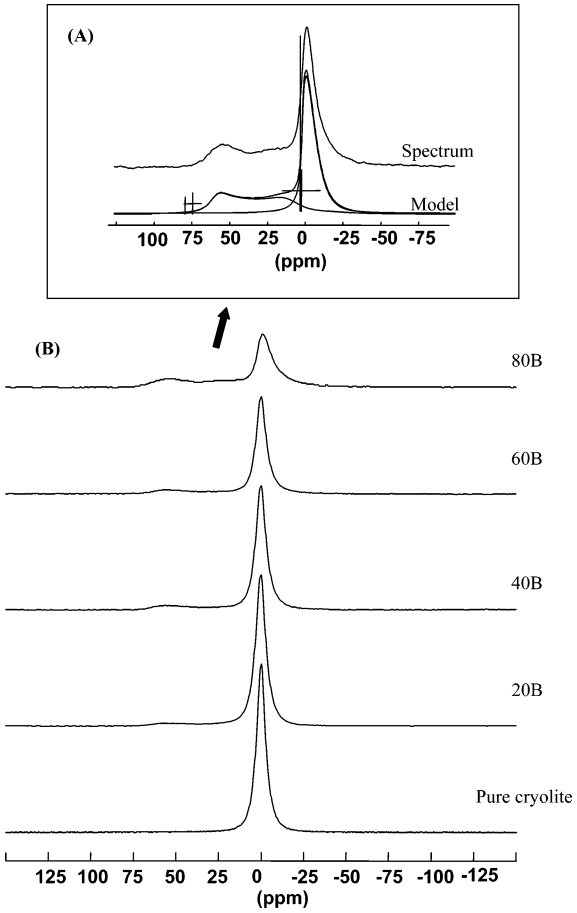

Figure 1. (A) Room temperature ^{27}Al fast MAS NMR spectra for the different $Na_2B_4O_7-Na_3AlF_6$ mixtures. (B) Spectrum and model for the 80 B sample.

This feature is also observed in the ^{23}Na spectra (Figure 2). Accordingly, the ^{23}Na spectrum of the 80 B mixture is similar to that of pure $Na_2O{\cdot}2B_2O_3$, showing the homogeneous insertion of cryolite in the glassy network.

Further additions of cryolite induce the superposition of two contributions originating from cryolite and $Na_2B_4O_7$, respectively. Chemical shifts (δ_{iso}) and QCC values for cryolite contribution are constant and equal to those reported in the pure material while in the case of the vitreous contribution, a slight shift of δ_{iso} toward higher values, from 3 to 13 ppm, was noticed on increasing Na_3AlF_6 content from 0 to 80%. In accordance with the correlation established by previous workers,[16,18] an increase in the ^{23}Na isotropic chemical shift can be associated with shorter average Na−O bond lengths. This observation is in good agreement with the modifier role of Na_3AlF_6 and a higher number nonbridging oxygen and/or fluorine atoms in the glassy network.

^{11}B MAS NMR spectra (Figure 3) show a partially resolved powder line shape, corresponding to BO_3 and BO_4 sites with an isotropic chemical shift at 21 and −0.5 ppm, respectively. The relative proportion of boron atoms with three and four ligands can be calculated by computer synthesis of their individual spectra. Thus, spectral simulation of a $Na_2O{\cdot}2B_2O_3$ glass gave 45% of boron atoms as BO_4 species within the glass. When the cryolite content is

(21) Massiot, D.; Fayon, F.; Capron, M.; King, I.; Le Calvé, S.; Alonso, B.; Durand, J.-O.; Bujoli, B.; Gan, Z.; Hoatson, G. *Magn. Reson. Chem.* **2002**, *40*, 70−76.
(22) Massiot, D.; Müler, D.; Hübert, Th.; Scheider, M.; Kentgens, A. P. M.; Coté, B.; Coutures, J.-P. *Solid State Nucl. Magn. Reson.* **1995**, *5*, 175−180.
(23) Simon, S.; Van Moorsel, G. J. M. P.; Kentgens, A. P. M.; De Boer, E. *Solid State Nucl. Magn. Reson.* **1995**, *5*, 163−173.

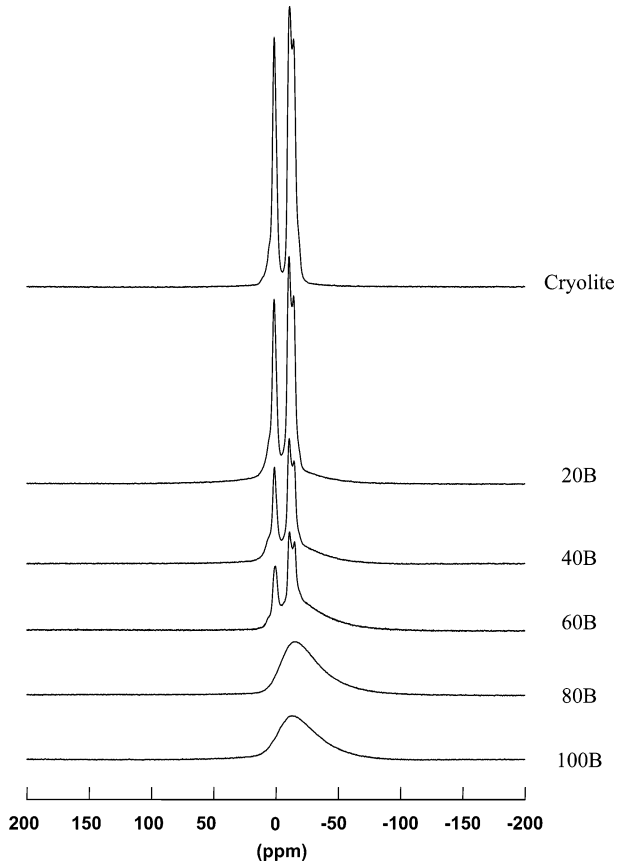

Figure 2. ^{23}Na fast MAS NMR spectra evolution at room temperature with Na_3AlF_6 contents.

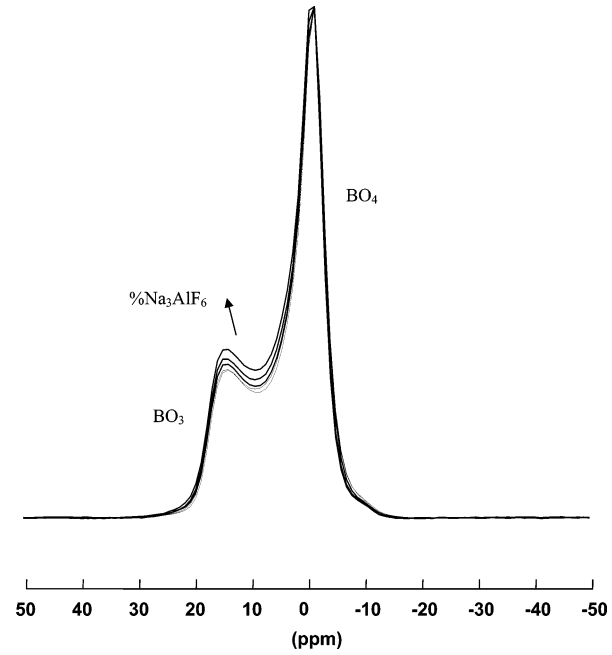

Figure 3. ^{11}B fast MAS NMR spectra for different $Na_2B_4O_7-Na_3AlF_6$ mixtures.

increased, this B_{III}/B_{IV} ratio is augmented, as a result of the depolymerization effect of cryolite on the borate network increasing the number of BO_3 species or new $B(O,F)_3$. To explain this process, we must take into account the AlF_6^{3-}

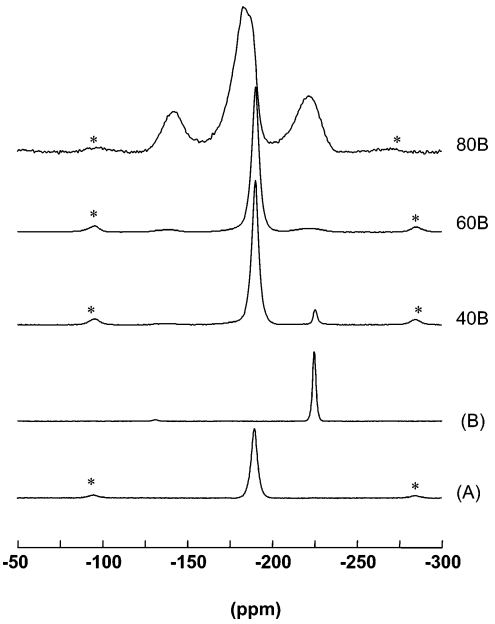

Figure 4. ^{19}F fast MAS NMR spectra of $Na_2B_4O_7-Na_3AlF_6$ mixtures. The spectra of pure cryolite (A) and NaF (B) are reported on the same figure for comparison. Spinning sidebands are marked with asterisks.

dissociation in the melts[13,14] and the formation of oxyfluoro species, as follows:

$$AlF_6^{3-} \rightarrow AlF_x^{(x-3)-} + (6-x)F^- \ (x = 4-6) \qquad (1)$$

$$BO_4 + yF^- \rightarrow B(O,F_y)_4 + (4-y)NBO \qquad (2)$$

$$AlF_x^{(x-3)-} + NBO \rightarrow AlF_{x-z}O_z^{(x+z-3)-} + zF^- \qquad (3)$$

where NBO means nonbridging oxygen, y is between 1 and 4, and z is less than 6.

While the 4-fold coordinated boron atoms tend to increase the number of fluorine ligands at the expense of oxygens, aluminum atoms seem to prefer oxygen atoms as $Na_2B_4O_7$ content increases. In this way, the presence of AlO_4^- was clearly evidenced on the ^{27}Al MAS spectra. We note that the oxyfluoro species formed could contain one or two nonbridging fluorine atoms (NBF), according to Shelby's theory. The last step of depolymerization is described by gradual conversion of the B_{IV} atoms into B_{III}:

$$B(O,F)_4 \rightarrow B(O,F)_3 + NBO/NBF \qquad (4)$$

The ^{11}B line shapes should be strongly modified[9] if BO_2F structural units are present in the glass at room temperature, due to the dipolar interaction between boron and fluorine, while only a slightly dipolar broadening is expected for $B(O,F)_4$ units. However, we have not noticed a net modification of the NMR line shapes, expected as evidence for such species.

On Figure 4, we have reported the comparative development of the ^{19}F MAS spectra of various binary mixtures and the pure compounds NaF and Na_3AlF_6. Thus, the 40 B spectrum has two main components, corresponding to the cryolite ($\delta = -190$ ppm) and NaF ($\delta = -225$ ppm) signals, and a small broad peak which arises at around -140 ppm.

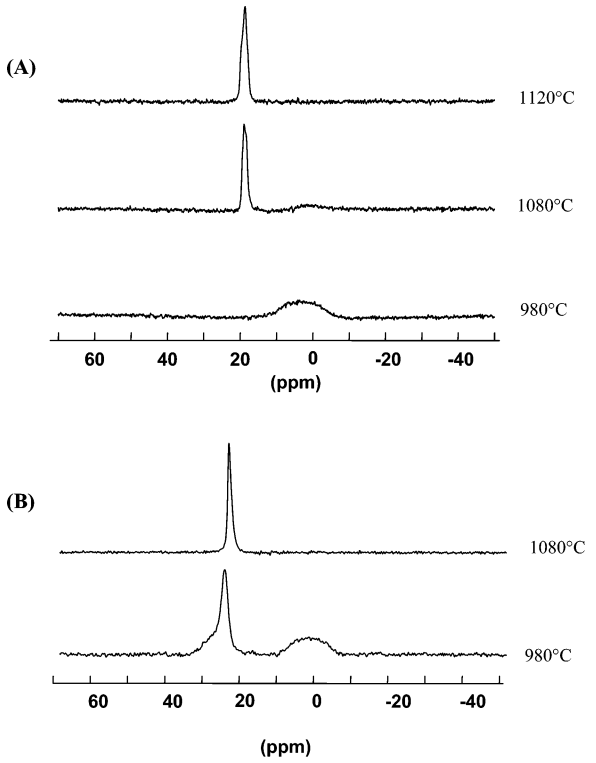

Figure 5. High temperature ^{27}Al NMR spectra of (A) pure Na_3AlF_6 and (B) 20 B mixture, over 980−1120 °C temperature range.

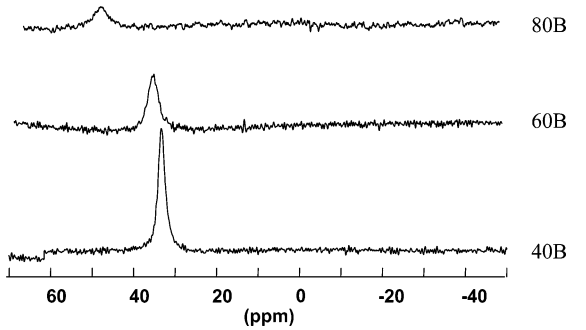

Figure 6. ^{27}Al HT NMR spectra of some binary $Na_2B_4O_7$−Na_3AlF_6 melts.

The intensity of the last contribution augments as the $Na_2B_4O_7$ content increases. As for the ^{19}F spectrum of the 80 B composition, all features are considerably enlarged due to the structural disorder existing in the glass. Moreover, the presence of the broad "NaF" signal confirms not only the formation of a small quantity of AlO_4^- species, previously mentioned for the ^{27}Al MAS spectrum, by means of reactions 1 and 3 but also the insertion of cryolite into the glassy network.

According to the data in the literature[10] the peak at about −140 ppm can be assigned to isolated terminal BOF_2 units strongly bonded to boron atoms. Instead, the absence of the lines at −162 and −120.8 ppm gives the evidence of the lack of BF_4 and BO_2F_2 groups into solidified mixtures.

Changes in the ^{27}Al, ^{23}Na, and ^{19}F chemical shifts show the insertion of (Al,F) species into the borate network. The increase in the BO_3 population can also be attributed to the insertion of the small fluorine content in the glass. In order

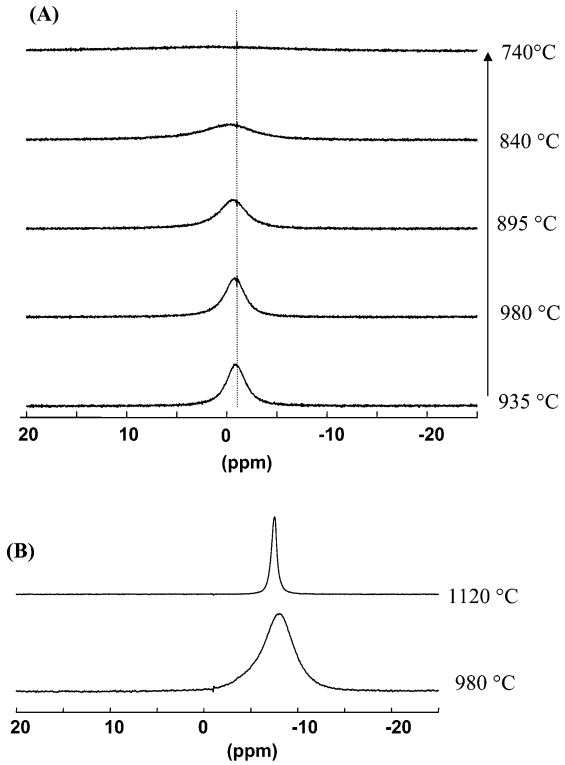

Figure 7. Temperature evolution of the ^{23}Na NMR spectra for: (A) $Na_2B_4O_7$ and (B) Na_3AlF_6.

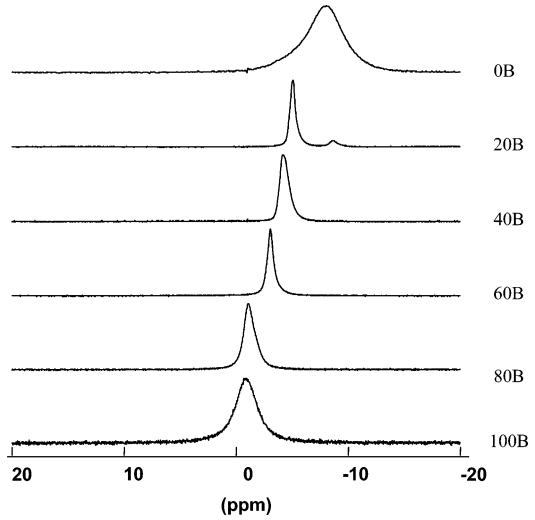

Figure 8. ^{23}Na HT NMR spectra of $Na_2B_4O_7$−Na_3AlF_6 melts.

to better understand the structural evolution in these melts, we now report in situ high temperature NMR measurements in liquids followed by spectral development with temperature and composition.

High Temperature NMR Spectra. High temperature static ^{27}Al spectra in molten $Na_2B_4O_7$−Na_3AlF_6 mixtures at 980 °C, illustrated in Figures 5 and 6, consist of a single line due to rapid exchange between the different species in the melt. The Lorentzian line shape shown indicates a complete dynamic averaging of the quadrupolar interaction, and the position of the lines is hence the weighted average of isotropic chemical shifts of the individual species.

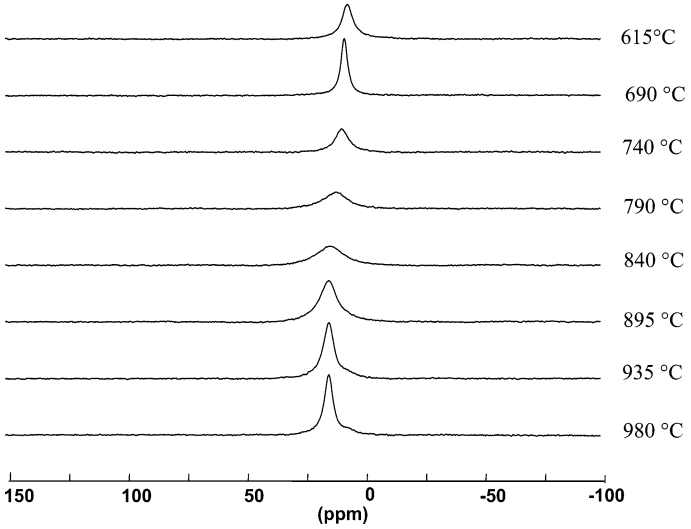

Figure 9. Temperature dependence of ^{11}B NMR spectra for 100B in the 615−980 °C temperature range.

Since cryolite and the 20 B mixture are not fully molten at 980 °C,[13,14] the high temperature solid phase (β) of cryolite, consisting of AlF_6^{3-} units, gives a broad signal at 3 ppm. Above the melting temperature, at 1080 °C, the spectrum of cryolite is now narrowed and shifted to 19 ppm, typical of a rapid exchange between the different possible coordinations AlF_x (where $x = 4-6$). Signals in net liquids, the ^{27}Al spectra of both cryolite and the 20 B mixture, are compared in Figure 5.

Variation in these chemical shifts, from 19 ppm for pure cryolite (Figure 6) up to 50 ppm for the binary mixture with 80% of $Na_2B_4O_7$, reveals a clear influence of the oxygen atoms on the aluminum environment, also pointed out by reaction 3.

The ^{23}Na spectra at 980 °C are illustrated in Figure 7 for pure cryolite and the diborate forming glass melt. As mentioned already, at 980 °C, since cryolite is in the β phase the signal is now broader than in the melt, with a chemical shift of −8.5 ppm, close to that of the melt, −7.5 ppm. In the glass, the peak position remains unchanged at −1 ppm over the whole temperature range. On cooling, the line is merely broadened, due to the increase in viscosity. The ^{23}Na spectra variation with melt composition shows a net shift toward lower chemical shift values, from −1 ppm in the glass forming melt $Na_2O{\cdot}2B_2O_3$ to −6 ppm in 20 B and −8 ppm in pure cryolite (Figure 8). This confirms the progressive substitution of oxygen by fluorine around sodium atoms in the melt.

The high temperature ^{11}B NMR spectra for $Na_2B_4O_7-Na_3AlF_6$ melts (Figure 9) show chemical shifts that can be treated as a weighted average of δ_{iso} corresponding to BO_3 and BO_4 species. At 980 °C, in the molten diborate (100 B), a chemical shift of 14.25 ppm would correspond to a BO_3/BO_4 ratio of 66:34 compared with 48:52 for the glass at room temperature. This behavior is clearly correlated with conversion of BO_4 units into BO_3 with a temperature increase, even in the absence of a modifier salt.

In order to avoid loss of cryolite by evaporation above 1000 °C, the maximum temperature we used was 980 °C.

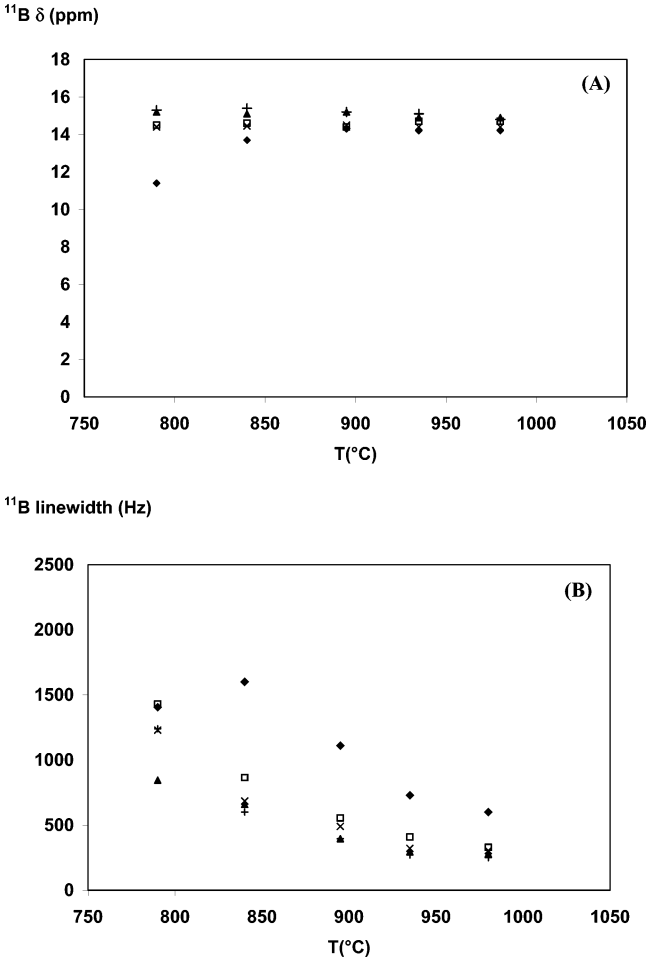

Figure 10. ^{11}B chemical shifts, δ_{iso}, (ppm) (A) and line widths (Hz) (B) with temperature evolution in the $Na_2B_4O_7-Na_3AlF_6$ melts. B100 (◆), B80 (□), B60 (×), B40 (+), B20 (▲).

Sen et al.[8] have studied borate, borosilicate, and boroaluminate liquids up to 1500 °C and reported temperature dependent changes above 1000 °C similar to the conclusions reached here but in absence of fluoride. Below 980 °C, we did not notice a shift in the position of the ^{11}B line in the

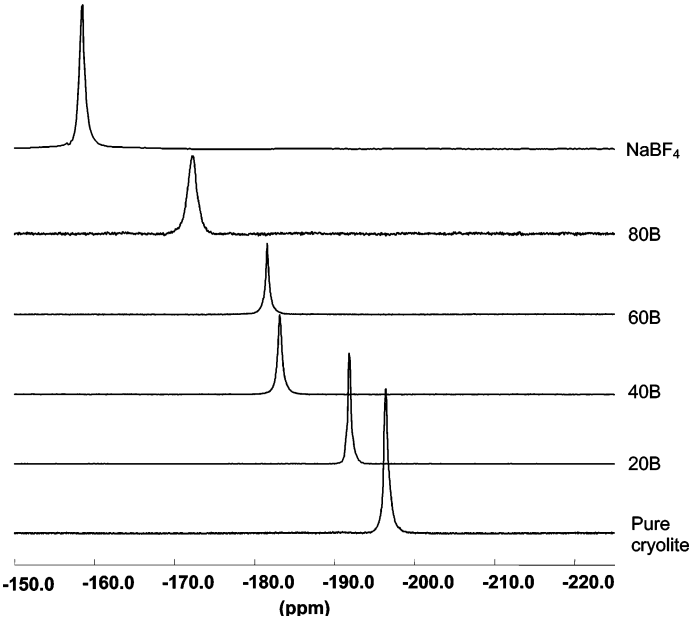

Figure 11. ^{19}F HT NMR spectra of $Na_2B_4O_7-Na_3AlF_6$ melts.

various compositions: the chemical shift stayed constant at 14.5 ppm. The change in structure is thus rather complex, and the fluorine present in the liquid must involve new species. Moreover, the influence of cryolite content on the spectra is also apparent on line width modifications (Figure 10). The 20 B binary mixture exhibits the narrowest line, which can be associated with weaker polymerized liquid and lower viscosity. Thus, at elevated temperature, reaction 4 can occur after the breaking up of large borate ring type units (diborate, tetraborate, and pentaborate units) containing B_{IV}. These high-membered boroxyl rings were earlier evidenced[5] by Raman spectroscopy to convert to 3-fold boron speciation in binary melts.

The ^{19}F spectra recorded in the binary melts (Figure 11) show the strong influence of boron atoms in the local environment of the fluorine atoms. Starting from pure molten cryolite at −190 ppm, the signal moves toward −172 ppm in 80 B, near the −158 ppm signal originating from the $NaBF_4$ melt where only the pure "Na,B" environment exists for fluorine. The same line enlargement observed for the other nuclei is clearly noticed in the case of the glass forming melt 80 B. This confirms the conclusions drawn from the observation of the other nuclei. However, the type of oxyfluoride species of either sp^2 or sp^3 boron atoms existing in the binary melts is still a matter for further structural investigations.

Conclusion

NMR investigations of the $Na_3AlF_6-Na_2B_4O_7$ system revealed the possible scenario of the devitrification process of a borate matrix to us. At first, glassy borate connectivity is weakened due to appropriate substitution of O^{2-} and F^- and formation of oxyfluoro species of boron atoms with one or two NBFs. Further, increasing $B(O, F)_3$ content was noted under the cryolite modifying effect. Moreover, large boroxyl rings are partially destroyed in favor of B_{III} speciation at elevated temperature.

Influence of oxygen atoms on the aluminum environment was evidenced not only on solidified samples, by formation of small amount of AlO_4^- groups, but also in melts.

Acknowledgment. This work has been financially supported by the EEC ARI Contract HPRI-CT-1999-00042 and CNRS-Romanian Academy cooperation.

IC026074O